

Search for Pauli Exclusion Principle Violation by Pair Production in the MAJORANA DEMONSTRATOR Calibration Data

I.J. Arnquist,¹ F.T. Avignone III,^{2,3} A.S. Barabash,⁴ C.J. Barton,⁵ K.H. Bhimani,^{6,7} E. Blalock,^{8,7} B. Bos,^{6,7} M. Busch,^{9,7} M. Buuck,^{10, a} T.S. Caldwell,^{6,7} Y-D. Chan,¹¹ C.D. Christofferson,¹² P.-H. Chu,¹³ M.L. Clark,^{6,7} C. Cuesta,¹⁴ J.A. Detwiler,¹⁰ Yu. Efremenko,^{15,3} H. Ejiri,¹⁶ S.R. Elliott,¹³ G.K. Giovanetti,¹⁷ M.P. Green,^{8,7,3} J. Gruszko,^{6,7} I.S. Guinn,^{6,7} V.E. Guiseppe,³ C.R. Haufe,^{6,7} R. Henning,^{6,7} D. Hervas Aguilar,^{6,7} E.W. Hoppe,¹ A. Hostiuc,¹⁰ M.F. Kidd,¹⁸ I. Kim,¹³ R.T. Kouzes,¹ T.E. Lannen V,² A. Li,^{6,7} A.M. Lopez,¹⁵ J.M. López-Castaño,^{3, b} E.L. Martin,^{6,7, c} R.D. Martin,¹⁹ R. Massarczyk,¹³ S.J. Meijer,¹³ T.K. Oli,⁵ G. Othman,^{6,7, d} L.S. Paudel,⁵ W. Pettus,^{20,21} A.W.P. Poon,¹¹ D.C. Radford,³ A.L. Reine,^{6,7} K. Rielage,¹³ N.W. Ruof,¹⁰ D. Tedeschi,² R.L. Varner,³ S. Vasilyev,²² J.F. Wilkerson,^{6,7,3} C. Wiseman,¹⁰ W. Xu,⁵ C.-H. Yu,³ and B.X. Zhu^{13, e}

(MAJORANA Collaboration)

¹*Pacific Northwest National Laboratory, Richland, WA 99354, USA*

²*Department of Physics and Astronomy, University of South Carolina, Columbia, SC 29208, USA*

³*Oak Ridge National Laboratory, Oak Ridge, TN 37830, USA*

⁴*National Research Center “Kurchatov Institute” Institute for Theoretical and Experimental Physics, Moscow, 117218 Russia*

⁵*Department of Physics, University of South Dakota, Vermillion, SD 57069, USA*

⁶*Department of Physics and Astronomy, University of North Carolina, Chapel Hill, NC 27514, USA*

⁷*Triangle Universities Nuclear Laboratory, Durham, NC 27708, USA*

⁸*Department of Physics, North Carolina State University, Raleigh, NC 27695, USA*

⁹*Department of Physics, Duke University, Durham, NC 27708, USA*

¹⁰*Center for Experimental Nuclear Physics and Astrophysics, and
Department of Physics, University of Washington, Seattle, WA 98195, USA*

¹¹*Nuclear Science Division, Lawrence Berkeley National Laboratory, Berkeley, CA 94720, USA*

¹²*South Dakota Mines, Rapid City, SD 57701, USA*

¹³*Los Alamos National Laboratory, Los Alamos, NM 87545, USA*

¹⁴*Centro de Investigaciones Energéticas, Medioambientales y Tecnológicas, CIEMAT 28040, Madrid, Spain*

¹⁵*Department of Physics and Astronomy, University of Tennessee, Knoxville, TN 37916, USA*

¹⁶*Research Center for Nuclear Physics, Osaka University, Ibaraki, Osaka 567-0047, Japan*

¹⁷*Physics Department, Williams College, Williamstown, MA 01267, USA*

¹⁸*Tennessee Tech University, Cookeville, TN 38505, USA*

¹⁹*Department of Physics, Engineering Physics and Astronomy, Queen’s University, Kingston, ON K7L 3N6, Canada*

²⁰*Department of Physics, Indiana University, Bloomington, IN 47405, USA*

²¹*IU Center for Exploration of Energy and Matter, Bloomington, IN 47408, USA*

²²*Joint Institute for Nuclear Research, Dubna, 141980 Russia*

(Dated: March 7, 2022)

The energy calibration data collected for the MAJORANA DEMONSTRATOR is used to search for a Pauli Exclusion Principle (PEP) violating process in an atomic system where a new fermion is introduced through the electron-positron pair production. The signature of this PEP violating process would be found through the cascade of a pair-produced electron to a forbidden atomic level of Ge. An improved limit on the parameter $\frac{1}{2}\beta^2$, which quantifies the probability of a PEP violating process, is measured to be $< 6.3 \times 10^{-4}$ at 95% CL for this process.

The Pauli Exclusion Principle (PEP) [1] is widely accepted in the scientific community but its physical cause is still unknown. This lack of knowledge has motivated theoretical development with small PEP violations and searches for indications of PEP-violating processes in a wide range of experiments. An extensive and thorough review, particularly from the experimental point of view, is found in [2]. In this paper, only the key points for the current analysis are described.

A search for a PEP violating atomic transition originating from a pair-produced fermion addresses the limitation of the super-selection rule due to the Messiah

and Greenberg symmetrization postulate [3]. The experimental effect of this rule is summarized by the Amado and Primakoff argument [4] which can be stated as: any fermion within a system that has already established its symmetry with respect to that system will not participate in a PEP-violating process even if the PEP is violated. As a consequence, the *newness* of a fermion to a given system for a given experimental configuration is critical to the interpretation of any PEP-violating process. As discussed in Ref. [2], many different experimental techniques have been employed with very different assumptions regarding this newness classification. Two experimental

strategies to add a fermion to a system include an electrical current through a source [5] and the creation of an electron through beta decay [6]. However, the strategy we pursue here, which is classified as a Type 1a fermion-system interaction, is to introduce a new electron from pair production (e_{pp}^-) as done in Ref. [2].

The term $\frac{1}{2}\beta^2$ is the ratio of a PEP-violating process to that of an equivalent process that obeys the PEP and therefore quantifies the probability of PEP violation. An advantage of the $\frac{1}{2}\beta^2$ parameter is that it provides a comparison between different PEP-violating processes of similar nature as it is not specific to just one process. In this work, we search for the $e_{pp}^- + Ge \rightarrow Ge$ PEP-violating process in the MAJORANA DEMONSTRATOR. In this notation, Ge represents a germanium atom and Ge is a germanium atom with an electron in a symmetric state. The best prior limit for this process is $\frac{1}{2}\beta^2 < 1.4 \times 10^{-3}$ at 99.7% CL [2] achieved by using a single high-purity germanium detector exposed to a ^{228}Th source. Here, the $\frac{1}{2}\beta^2$ limit is improved with the calibration data from the MAJORANA DEMONSTRATOR. The process is possible in the MAJORANA DEMONSTRATOR because it comprises an array of Ge detectors that are calibrated by a ^{228}Th radioactive source. The e_{pp}^- are produced by the 2614 keV γ ray from the decay of ^{208}Tl .

The MAJORANA DEMONSTRATOR [7] is an array of p-type, point-contact high-purity germanium detectors divided between two separate modules that share a common low-background shield. It was designed and operated to search for neutrinoless double-beta decay of ^{76}Ge [8, 9] and to demonstrate the feasibility of a ton-scale detector to further probe neutrinoless double-beta decay at smaller effective Majorana mass scales [10]. The low noise, low energy threshold, and excellent energy resolution of the MAJORANA DEMONSTRATOR array has additionally enabled a leading limit on the double-beta decay of ^{76}Ge to excited states [11] and searches for physics beyond the Standard Model [12–14].

The MAJORANA DEMONSTRATOR detectors are operated in vacuum cryostat within a graded shield made from ultra-low background electroformed Cu and other shielding materials sourced to meet the stringent material purity requirements [15]. A calibration system [16] introduces a ^{228}Th line source through a track that penetrates the shield and surrounds each cryostat in a helical shape. When fully deployed, the line source exposes all of the detectors in the array for energy calibration and stability determination. During normal operations, a source is deployed weekly for roughly an hour to perform routine energy calibrations, and again every few months for a 17-hr period to collect enough counts to tune analysis parameters (less than 3% of statistical uncertainty in the DEP). The primary operation of MAJORANA DEMONSTRATOR began in June 2015 and concluded in March 2021 while the calibration data used in this analysis spans September 2015 - November 2019.

The advantage of the MAJORANA DEMONSTRATOR over the previous best limit for PEP violation originating from pair-produced fermions [2] stems from its greater source of exposure, which translates to 20% more counts. This increase in counts comes from both the longer source run time and the larger mass of germanium (about 20 times higher) which compensates for the smaller detection efficiency.

We search for a rare PEP-violating process where a new fermion is introduced to an atomic system. To use the MAJORANA DEMONSTRATOR data for this search, we require 1) electron-positron pair production, 2) large statistics to observe a rare PEP-violating process, and 3) a clear separation between the PEP-violating signal and a PEP-allowed transition. The single-escape peak (SEP) and the double-escape peak (DEP) of the 2614 keV γ ray generated from ^{208}Tl decay to ^{208}Pb satisfies the requirements of introducing a new electron to the system. The SEP and DEP signatures are clearly observed above the energy continuum in the MAJORANA DEMONSTRATOR calibration data. If the PEP is violated, the pair-produced electron may be captured and transition to the occupied K shell of a Ge atom. The energy of this x-ray emission will sum with the SEP or DEP peak producing a PEP-forbidden peak at a slightly higher energy than the PEP-allowed peak. The transition energy of this forbidden process was calculated in Ref. [2] to be 10.6 keV when correcting for the additional shielding of the nuclear charge when the K shell is occupied. The signature of the PEP-forbidden transition is a peak at an energy 10.6 keV higher than the PEP-allowed single- or double-escape peaks. The probability for this PEP-violating process is given in (1), where N_e is the number of events in the PEP-forbidden peak and N_M is the number of events in the PEP-allowed escape peak.

$$\frac{1}{2}\beta^2 = \frac{N_e}{N_M} \quad (1)$$

The number of events in the single- or double-escape peaks are measured from the MAJORANA DEMONSTRATOR calibration single-detector hit spectrum shown in Fig. 1. The peak-fitting method used to extract the number of events is described later in this document with several analysis methods used depending on which of the two escape peaks are being fit. In the SEP (DEP) method, the SEP (DEP) is fit to determine $\frac{1}{2}\beta^2$. Additionally, the fit can combine the energy ranges to fit both peaks at the same time in what is called the SEP+DEP method. This analysis method simultaneously performs the SEP and DEP fits while constrained to keep a common $\frac{1}{2}\beta^2$ between the two. The SEP+DEP method combines the statistics of the individual SEP and DEP methods and if the systematic uncertainty is significantly smaller than the statistical uncertainty, this method will provide the best possible result. To the contrary, if the statistical

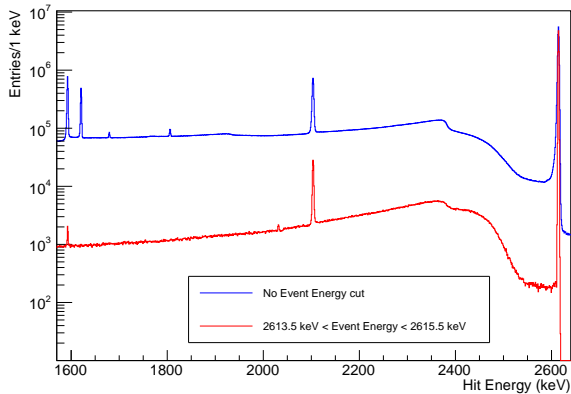


FIG. 1. Detector hit spectrum for ^{228}Th calibration data in the MAJORANA DEMONSTRATOR (blue) and the same spectrum when the total event energy summed over multiple detectors is within the range of the 2614.5 keV full γ ray energy (red).

TABLE I. Energy range for fitting in the hit spectrum, energy range of the PEP-forbidden peak in the hit spectrum, allowed energy loss from the 2614.5 keV γ in the event, and bin size for each analysis method in which only one escape peak is fit.

Condition\method	SEP	SEP- γ	DEP
Hit Energy (keV)	[2099.5 – 2132]		[1585 – 1607.6]
Peak Energy (keV)	[2110.1 – 2118.1]		[1599.9 – 1606.3]
Energy lost (keV)	≤ 511	0	≤ 1022
Bin size (keV)	0.01	0.1	0.01

uncertainty is much lower than the systematic uncertainty, an energy spectrum with a much lower signal-to-background ratio would produce a more stringent $\frac{1}{2}\beta^2$ limit. Such a spectrum is constructed by adding the condition that the event energy of all detectors sums to the full γ ray energy (2614.5 keV) to ensure there was no energy loss. This event energy spectrum is shown as a red line in Fig. 1. In this method, only the SEP peak is visible and it is referred to as the SEP- γ method. Each one of the four methods described previously (SEP, DEP, SEP+DEP and SEP- γ) uses a spectral fit to provide the estimation of $\frac{1}{2}\beta^2$. The four analysis methods are constrained over different energy ranges due to the peak energy location and separate energy binning due to their varying count rates. The energy range of the fit, bin size, PEP-forbidden peak, and the energy loss for the 2614 keV γ for each single analysis method (SEP, DEP and SEP- γ) are listed in Table I.

The analysis of a peak on a continuum requires appropriate binning of the data to achieve a proper fit. The binning for the prominent escape peaks is chosen such that the Poisson uncertainty of each bin is less than 5%, the bin energy scale is an integer power of 10, and the number of bins is as high as possible. For the analysis of the faint (or nonexistent) PEP-forbidden peak, a

TABLE II. Best fit parameters for the SEP and SEP- γ analysis methods.

Parameter	SEP	SEP- γ
$(1/2)\beta^2$	0	0
N_M (counts)	33340	18250
μ (keV)	2103.5	2103.5
σ (keV)	1.92	1.938
f	0.133	0
τ (keV)	2.5	-
H (counts)	0	0
m (counts/keV)	0.31	0.58
n (counts)	210	-841

multi-bin peak fit is not optimal because the shape of the peak is hidden within the Poisson uncertainty of the background. For that reason, a simple counting analysis is performed over the full energy range of the PEP-forbidden peak to determine the amplitude of that peak. The counting analysis is included in the overall fit by treating the energy range of the PEP-forbidden peak as a single bin in the fit, as listed in Table I. The PEP-forbidden peak single-bin width is chosen to cover a 5σ region around the expected PEP-forbidden peak mean, where σ comes from the standard energy resolution obtained in Ref. [9]. The choice of 5σ is sufficient to statistically ensure a probability of finding a count due to a PEP-violating process outside the considered energy region to be effectively zero. Given a background with a statistical fluctuation of hundreds of counts, a probability of finding a PEP-violating count of 3×10^{-7} is negligible and consistent with the likelihood construction as the Eqn. 6.

Likelihood Fit.— The $\frac{1}{2}\beta^2$ parameter is determined through a binned likelihood fit of the detector hit energy spectrum. The model used to fit the spectrum includes a linear background and two peaks; the main escape peak is described by the MAJORANA peak shape routine [9] while the higher energy PEP-forbidden peak is fully contained in a single bin with no shape needed. The linear background is defined by the slope (m) and y-intercept (n). The shape of the main peak has a Gaussian component defined by a mean (μ) and a width (σ); a low energy exponential tail contribution defined by the same mean, width, and an exponential slope (β); and a background step function defined by the same mean and width with a step height (H). The fraction of the signal events that are in the tail (f) also defines the overall peak shape. The full peak shape is normalized to the number of events in the main escape peak (N_M). The number of events in the PEP-forbidden peak is $N_e = (1/2)\beta^2 \cdot N_M$. Finally, the SEP+DEP method uses two separate energy regions and as a consequence, all previous variables are duplicated and indicated by the subscript r to denote the region.

The binned likelihood (\mathcal{L}) function used in the fit is given in Eqn. (2), where i refers to an energy spectral bin, θ makes reference to all the nuisance parameters as

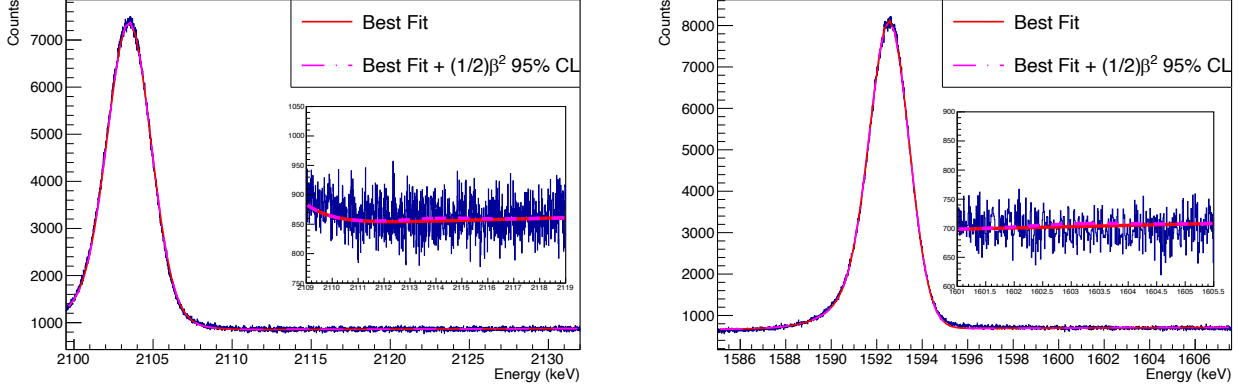


FIG. 2. Best fit for the SEP+DEP analysis method (red) over the SEP (left) and DEP (right) energy regions. A limit on $\frac{1}{2}\beta^2$ at the 95% CL is also included (pink-dashed).

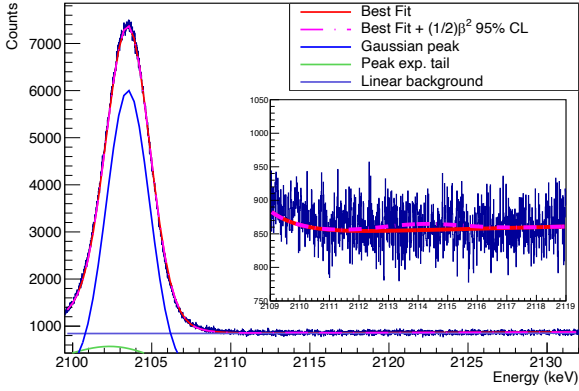


FIG. 3. Best fit to the SEP energy region for the SEP analysis method (red). The different non-zero contributions to the model are included: linear background (purple), Gaussian peak (blue), and low energy tail (green). A limit on $\frac{1}{2}\beta^2$ at the 95% CL is also included (pink-dashed).

TABLE III. Best fit parameters for the DEP analysis methods.

Parameter	DEP
$(1/2)\beta^2$	0
N_M (counts)	23300
μ (keV)	1592.6
σ (keV)	1.20
f	0.14
τ (keV)	1.02
H (counts)	0
m (counts/keV)	2.47
n (counts)	-3240

given in Eqn. 3, \mathcal{L}_i is the likelihood for the entries in this bin, and \mathcal{L}_{pull} are pull terms to include available information regarding parameters μ . This \mathcal{L}_{pull} term is defined in Eqn. (4), where index $\bar{\mu}$ is the expected value of the

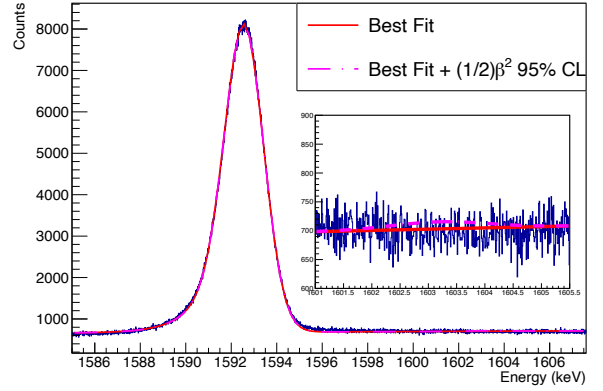


FIG. 4. Best fit for the DEP energy region in the DEP analysis method (red). A limit on $\frac{1}{2}\beta^2$ at the 95% CL is also included (pink-dashed).

escape peak that is being fitted and σ_μ is the uncertainty of that expected value. The \mathcal{L}_i term is the product of the Poisson probability of finding the observed number of events in a bin when the expected value is that found by the model. This term appears in Eqn. 5, where index i indicates the bin, P is the Poisson probability, \mathcal{O}_i is the number of events observed in the bin i , \mathcal{M} is the expected number of events in the bin according to the model, and j is a parameter which enables the contribution of $\frac{1}{2}\beta^2$: $j = 1$ over the energy range of the PEP-forbidden peak and $j = 0$ otherwise. The expected model events in the bin, \mathcal{M} , is defined in Eqn. 6, where E_i is the energy of the center of the bin, \mathcal{P} is the MAJORANA peak shape function including the linear background, and \int_i indicates that the integral is calculated between the bin limits.

$$\mathcal{L} = \prod_r \prod_i \mathcal{L}_i \left(\frac{1}{2}\beta^2, \theta \right) \mathcal{L}_{pull}(\mu_r) , \quad (2)$$

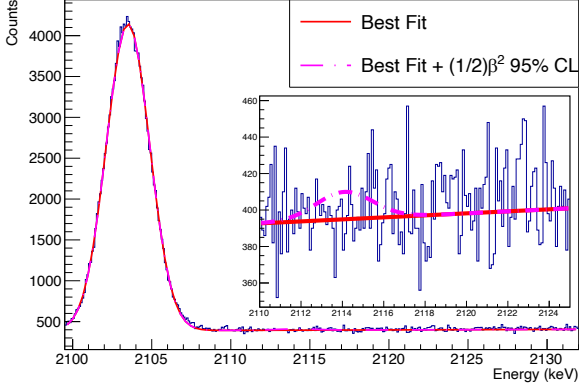


FIG. 5. Best fit for the SEP energy region for the SEP- γ analysis method (red). A limit on $\frac{1}{2}\beta^2$ at the 95% CL is also included (pink-dashed).

$$\theta = (N_{M-r}, \mu_r, \sigma_r, \beta_r, f_r, H_r, m_r, n_r) \quad (3)$$

$$\mathcal{L}_{pull}(\mu) = \frac{1}{2\pi} \prod_p \frac{e^{-\frac{\mu - \bar{\mu}}{\sigma_\mu}}}{\sigma_\mu} \quad (4)$$

$$\mathcal{L}_i\left(\frac{1}{2}\beta^2, \theta\right) = \prod_i P(\mathcal{O}_i | \mathcal{M}(j, \theta)) \quad (5)$$

$$\mathcal{M}(j, \theta) = j\frac{1}{2}\beta^2 N_M + \int_i \mathcal{P}(\theta) dE \quad (6)$$

Prior to performing the likelihood fit, an initial fit of a simple Gaussian plus a linear background is performed by using ROOT [17]. The results of this fit are used as initial values in the likelihood fit, while the error in the Gaussian mean is used to estimate $\Delta\mu$. The initial values of the free parameters are set to be $\beta_r = 1.7$, $f_r = 0.15$ and $H_r = 0$, where the two first values are obtained as an average of the fits for the resolution of each dataset [9].

Results.— The results of the best fit obtained from the initial conditions using the likelihood fit of Eqn. (2) are shown in Tables II and III for single methods. As the SEP and DEP methods coincidentally have the same value of $\frac{1}{2}\beta^2$, the combined SEP+DEP fit has the same central values of the SEP method in the SEP region and the DEP method in the DEP region, while the CL interval will be different. Figure 2 shows the fit result in both energy regions for the combined method, while Fig. 3, 4, 5 show the fits for the individual methods. Figure 3 additionally shows the non-zero contributions of the MAJORANA peak shape.

The best fit to the energy spectrum for each analysis method provides the central values of each parameter, which is determined by finding the minimum of the negative logarithmic likelihood function. This function is also used to determine the CL intervals by calculating the difference between its minimum and its value over a range of the parameter of interest, which is called Δ log-likelihood. All $\frac{1}{2}\beta^2$ values where Δ log-likelihood is lower than 1.96 establishes the 95% CL interval. The Δ log-likelihood distributions for the SEP, SEP- γ , DEP, and SEP+DEP analysis methods are shown in Fig. 6. These distributions are constructed by using a conservative approach in which the Δ log-likelihood minimum is not constructed from the nuisance parameters provided by the best fit. Instead, the nuisance parameters are varied by $\pm 1\sigma$. From all the possible combination of nuisance parameter values obtained this way, the one that produces the largest Δ log-likelihood is used to estimate the limits. This latter method is intended to include systematic errors in the analysis and represents the final limits on PEP violation given in Table IV. The best upper limit of $\frac{1}{2}\beta^2 < 6.3 \times 10^{-4}$ (95% CL) comes from the SEP+DEP analysis method.

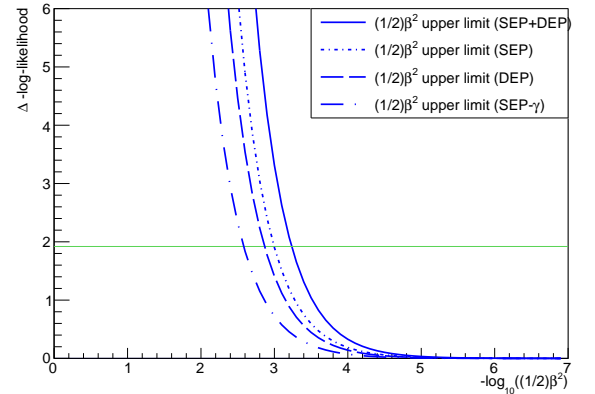


FIG. 6. Log-likelihood after subtraction of the log-likelihood minimum versus $(1/2)\beta^2$ for SEP, DEP, SEP- γ and SEP+DEP methods as the legend indicates. The green line indicates the 95% CL value

TABLE IV. $(1/2)\beta^{1/2}$ upper limits from each method. The best limit is indicated in bold.

method	95%CL	3σ
SEP	1.3×10^{-3}	1.6×10^{-3}
DEP	1.6×10^{-3}	2.1×10^{-3}
SEP- γ	2.7×10^{-3}	4.0×10^{-3}
SEP + DEP	6.3×10^{-4}	1.0×10^{-3}

This result improves the limit on PEP-violating search based on a new electron generated from electron-positron pair-production introduced within a high-purity germanium detector. The previous best limit on the reaction

$e_{pp}^- + Ge \rightarrow Ge$ is 1.4×10^{-3} at 3σ [2]. This work improves these results for the same PEP-violating process through the additional source exposure collected by the MAJORANA DEMONSTRATOR to a leading upper limit of 6.3×10^{-4} at the 95% CL (1.0×10^{-3} at 3σ). In the future, the LEGEND experiment [10] will further enhance the strengths of the MAJORANA DEMONSTRATOR experiment. LEGEND will search for the same PEP-violating process with an even larger data set, allowing for a potential improvement this limit.

This material is based upon work supported by the U.S. Department of Energy, Office of Science, Office of Nuclear Physics under contract / award numbers DE-AC02-05CH11231, DE-AC05-00OR22725, DE-AC05-76RL0130, DE-FG02-97ER41020, DE-FG02-97ER41033, DE-FG02-97ER41041, DE-SC0012612, DE-SC0014445, DE-SC0018060, and LANLEM77/LANLEM78. We acknowledge support from the Particle Astrophysics Program and Nuclear Physics Program of the National Science Foundation through grant numbers MRI-0923142, PHY-1003399, PHY-1102292, PHY-1206314, PHY-1614611, PHY-1812409, PHY-1812356, and PHY-2111140. We gratefully acknowledge the support of the Laboratory Directed Research & Development (LDRD) program at Lawrence Berkeley National Laboratory for this work. We gratefully acknowledge the support of the U.S. Department of Energy through the Los Alamos National Laboratory LDRD Program and through the Pacific Northwest National Laboratory LDRD Program for this work. We gratefully acknowledge the support of the South Dakota Board of Regents Competitive Research Grant. We acknowledge support from the Russian Foundation for Basic Research, grant No. 15-02-02919. We acknowledge the support of the Natural Sciences and Engineering Research Council of Canada, funding reference number SAPIN-2017-00023, and from the Canada Foundation for Innovation John R. Evans Leaders Fund. This research used resources provided by the Oak Ridge Leadership Computing Facility at Oak Ridge National Laboratory and by the National Energy Research Scientific Computing Center, a U.S. Department of Energy Office

of Science User Facility. We thank our hosts and colleagues at the Sanford Underground Research Facility for their support.

^a Present address: SLAC National Accelerator Laboratory, Menlo Park, CA 94025, USA

^b Corresponding author. Email: lopezcastajm@ornl.gov

^c Present address: Duke University, Durham, NC 27708

^d Present address: Institute for Experimental Physics; Universität Hamburg; Luruper Chaussee 149; 22761 Hamburg, Germany

^e Present address: Jet Propulsion Laboratory, California Institute of Technology, Pasadena, CA 91109, USA

- [1] W. Pauli, Z. Phys. **31**, 765 (1925).
- [2] S. R. Elliott, B. H. LaRoque, V. M. Gehman, M. F. Kidd, and M. Chen, Found. Phys. **42**, 1015 (2012).
- [3] A. M. L. Messiah and O. Greenberg, Phys. Rev. **136**, B248 (1964).
- [4] R. D. Amado and H. Primakoff, Phys. Rev. C **22**, 1338 (1980).
- [5] E. Ramberg and G. A. Snow, Physics Letters B **238**, 438 (1948).
- [6] M. Goldhaber and G. Scharff-Goldhaber, American Physical Society **73**, 1472 (1948).
- [7] N. Abgrall and others (MAJORANA), Adv. High Energy Phys. **2014**, 365432 (2014).
- [8] N. Abgrall and others (MAJORANA), Phys. Rev. Lett. **120**, 132502 (2018).
- [9] S. I. Alvis and others (MAJORANA), Phys. Rev. C **100**, 025501 (2019).
- [10] N. Abgrall *et al.* (LEGEND), (2021), [arXiv:2107.11462](https://arxiv.org/abs/2107.11462) [physics.ins-det].
- [11] J. I. Arnuist and others (MAJORANA), Phys. Rev. C **103**, 015501 (2021).
- [12] N. Abgrall and others (MAJORANA), Phys. Rev. Lett. **118**, 161801 (2017).
- [13] S. I. Alvis and others (MAJORANA), Phys. Rev. Lett. **120**, 211804 (2018).
- [14] S. I. Alvis and others (MAJORANA), Phys. Rev. D **99**, 072004 (2019).
- [15] N. Abgrall and others (MAJORANA), Nucl. Instrum. Meth. A **828**, 22 (2016).
- [16] N. Abgrall and others (MAJORANA), Nucl. Instrum. Meth. A **872**, 16 (2017).
- [17] R. Brun *et al.*, <https://root.cern>.